CFD simulation of Earth Duct connected to double brick wall system on indoor airflow in model with symmetric opening position (traditional passive cooling system in the north of Iran)

Mina Lesan[1], Maryam Lesan[2]
[1, 2] *Iran University of Science and Tecnology, Tehran, Iran*
lesan@alumni.iust.ac.ir
[2] *Nooshirvani university of science and technology, Babol, Iran*
m.lesan@nit.ac.ir

Abstract: Passive systems for natural ventilation design have the ability to control the mechanism of wind in order to improve indoor conditions. Many of the previous studies have focused on analyzing different parameters and passive systems to predict the indoor natural airflow. Building parameters and systems are important in determining the feasibility of natural ventilation design. In an urban scale, traditional buildings in the north of Iran used the passive cooling system which is called breezeway (Nafas Kesh) in order to make buildings more breathable and cool the internal spaces. This study focuses on the performance of the earth duct connected to a double brick wall (breezeway) system and the impact of different breezeway width on indoor natural ventilation. This system was simulated by computational fluid dynamics (CFD) program. A model with fixed earth duct height of 0.01 in reduced scale and different breezeway widths of 0.008 m and 0.02 m and 0.04 m in 1:200 reduced scale was analyzed. Results show that model with fixed earth duct height of 0.01 m connected to breezeway widths of 0.08 m and 0.02 m decreases indoor volume flow rate 10% and 4%, respectively. While the model with breezeway width of 0.04 m increases indoor flow rate slightly equal to 2%. In a model with breezeway widths of 0.008 m and 0.02 m Indoor mean air velocity decreases 30% and 10%, respectively. Although in model with breezeway width of 0.04 the mean air velocity increases 3%.
Keywords: Natural ventilation, breezeways, earth ducts, CFD.

1. Introduction

The wind has played a great role in architecture in hot and humid seasons. Air movement makes human feel cooler and conditions the indoor spaces better under a hot and humid environment. Thus, natural ventilation serves as the most effective passive design strategy for hot and humid regions. Buildings develop in order to adapt to their climate. Decisions which respond to climate, make their mark in design. Considering the vernacular architecture in the north of Iran, the vernacular buildings were designed on stilts with elevated floors in order to take the full advantage of the prevailing wind. Holmes (1994) found out Building which has an elevated floor, the effect on natural ventilation in a positive way. In urban scale, the vernacular buildings on stilts are located near the backyard brick wall which mostly has a width of 1m and called breezeway (Nafas kesh). The breezeway is connected to a raised-up floor (crawl space) under the building and mostly made up of two brick walls. In this type of buildings, the air passes under the raised-up floor and exits from the breezeway (Figure 1). Therefore, this system affects indoor natural ventilation and airflow. Many previous researchers have studied the effect of different parameters and systems on natural ventilation in vernacular buildings. Similar to other parameters, breezeway at the backyard of buildings could also affect indoor

Revisiting the Role of Architecture for 'Surviving' Development. 53rd International Conference of the Architectural Science Association 2019, Avlokita Agrawal and Rajat Gupta (eds), pp. 51–60.

natural ventilation. Therefore, it is an important measure to take into account. The geometry of breezeways at building backyards can increase or decrease indoor natural ventilation. The purpose of this paper is to study the effect of breezeway shaft depth on indoor airflow. Computational Fluid Dynamics is a powerful tool for studying natural ventilation and was used as a data collection tool in this study.

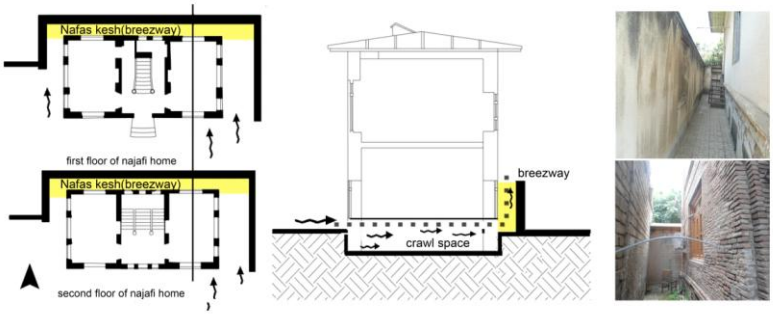

Figure 1: Breezeway at the backyard in urban scale vernacular buildings in north Iran.

2. Literature review

The range of vernacular low-rise buildings in hot and humid climates have several notable characteristics which have an effect on natural ventilation. These characteristics are defined in four major groups: 1) pitch roofs, 2) large openings, 3) elevated floors, 4) building aspect ratio. There are some studies within group 1 including gable-roof, arched roofs and shed roofs. Holmes (1994) found out mean pressure difference between windward and leeward facades increases by

increasing pitch angle in gable roofs. Tomingaa et al. (2015) studied three different pitch gable roofs and pointed out the flow pattern around the building changes critically around 20% at the pitched roof. Holmes (1994) compared gable roof of 18" pitch with a hip roof which was studied by Meecham et al. (1991) and found out the highest pressures on the hip roof were significantly less than those on gable roof of the same pitch. Holmes(1994) also found out by increasing roof elevation, external mean pressure on building increases. Chu and Chiang (2014) found out building aspect ratio affect indoor natural ventilation. they found out by increasing the depth of the building, the pressure difference decreases. They found out the best depth to height ratio is less than 5. The information from these studies is important to those choosing pressure coefficients for ventilation design.

Peren et al. (2015) pointed out that indoor natural ventilation increases in shed roof with asymmetric opening positions. Chu and Chiang (2014) suggested that the ventilation process in openings in opposite corners of the windward and leeward facades was 15.5% lower than that of openings on the centerline of buildings. Tominaga and Blocken (2015) found out buildings without shelter have 30% more natural ventilation.

Some researchers studied on the effect of detail component designs on natural ventilation. Peren et al. (2015) worked on the impact of eaves on indoor natural ventilation and found out both windward and leeward eaves result in an increase of volume flow rate and windward eaves with an inclination of 27' (equal with a roof angle) result in the highest increase of volume flow rate. Kosutova et al. (2019) worked on isolated building equipped with louvers and found out that louvers at the upper part of the façade had the most indoor airflow rate compare to lower and middle openings without. Montazeri and Blocken (2013) studied pressure distribution as an important factor parameter for natural ventilation on a building with and without balconies. They found out it can cause significant changes in pressure distribution, as much as 30% in some areas. Tantasavasdi et al. (2001) found out it is better to use square-shaped plan than rectangular for natural ventilation. Therefore, in this study, a cubic model was chosen as a base model and then investigated.

Three types of measurements can be used to study natural ventilation: scale model, wind tunnel measurements, and full-scale measurements. Computational fluid dynamics (CFD) is a powerful approach to study natural ventilation. Experimental measurements can give much more accurate results than analytical models. Many

building parameters and systems were investigated in previous studies. The review of the literature shows that almost no studies have been conducted on the effect of building on stilts integrated to breezeway shaft on indoor natural ventilation. Therefore, this study investigates the effect of different breezeway width on indoor airflow pattern and volume flow rate in an elevated floor building with symmetric opening positions using computational Fluid Dynamics. CFD is one of the most powerful software in predicting indoor airflow. All of the simulations were performed using ANSYS Fluent 12. The experimental data breezeway used to validate the numerical data which was performed by Karava (2008).

3. Methodology

Experimental measurements are described in subsection 3.1. The numerical model based on experimental data for validation is presented in subsections 3.2. After a good agreement between experimental data and numerical data from simulations, section 4 presents the CFD simulation results for the models without the breezeway shaft and with the three different breezeway shafts base on 0.01 height elevated floor. Discussions and conclusions are given in section 5. Wind tunnel experiment was used to provide accurate flow data for validating the results of computer simulation. The experimental model which was used for verification and validating of the numerical model is described in the following section.

3.1. Wind tunnel experiment model

The experimental data by Karava (2008) was used to validate the numerical data. A small-scale cubic model (1:200), 0.1 m × 0.1 m × 0.08 m (W×D×H) was constructed out of 2mm cast transparent Polymethyl methacrylate (PMMA). The scale model was corresponding to dimensions of 20 m× 20 m × 10 m (W×D×H) in full scale. The studied models had three different wall porosities 5%, 10% and 20% with three different opening positions at the bottom, middle and top in both windward and leeward facade. The PIV measurements for an isolated building model was carried out in wind tunnel of Concordia University, Canada. The mentioned wind tunnel is open-circuit boundary layer wind tunnel with a test section of 1.8 × 1.8 × 12 m^3. The mean wind speed and turbulence intensity were measured 6.97 m/s and 10%, respectively at the building model height. For more information related to the experimental data which was used in this study, the reader is referred to the Karava (2008). In this study, the focus is on the reduced scale experimental model with symmetric opening positions at the middle of the windward and leeward façade and with wall porosity of 10%. The center of the opening is 40mm height at both windward and leeward façade. The size of each opening was 0.046 m × 0.018 m (length × height) (Figure2). The defined AB line at the middle of the windward and leeward opening (40mm) used for comparisons in simulations.

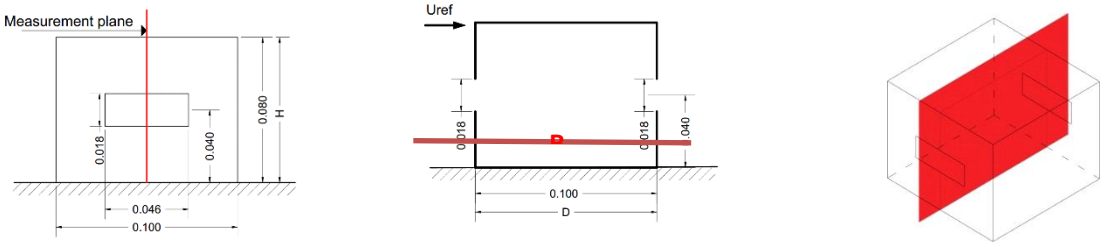

Figure2: Front, section and perspective view of the reduce-scale experimental model studied by Karava et al. (2008) used for numerical simulation.

3.2. CFD model description

3.2.1. Boundary condition

In order to replicate the experimental wind tunnel measurements performed by Karava (2008), building geometry was modeled in a computational domain. The computational domain was modeled base on the best practice guidelines by Franke et al. (2007) and Tominaga et al. (2008). The outer computational domain had an upstream length of 3H, a downstream of 15H, a lateral length of 3H on both sides of the building, and a vertical

length of 3H above the building height. The domain size was 0.9 m × 0.48 m × 1.54 m in a 1:200 reduced scale, which corresponds to 180 × 308 × 96 m^3 in full scale. Figure 3.a indicates the computational domain.

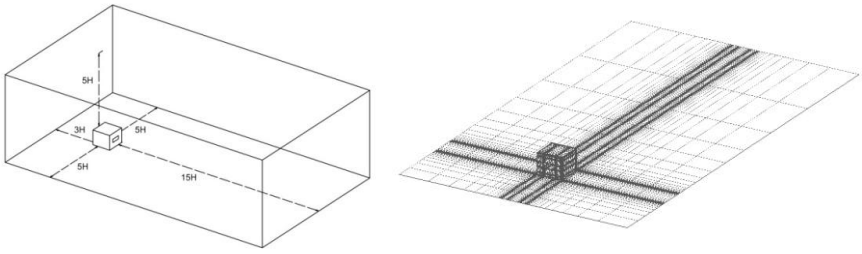

Figure 3: Perspective view of a building model in the computational domain.

Three meshes, course with 456192 cells, basic with 773936 cells, and fine with 1617840 cells, were applied for grid independence test (Figure 4). The mesh density is increase near the openings. Grid independence tests indicate mesh size with 773936 cells are sufficient for the model (Figure 5). The Building geometry was constructed by Gambit software. The mesh was fully structured.

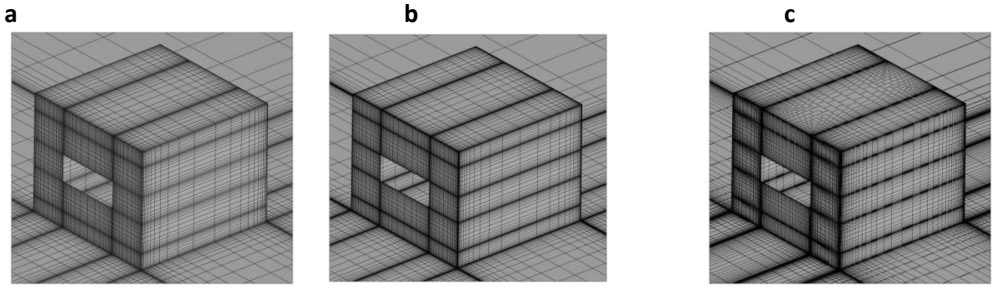

Figure 4: View of computational grid.a.coarse grid, b.basic grids and c. fine grid

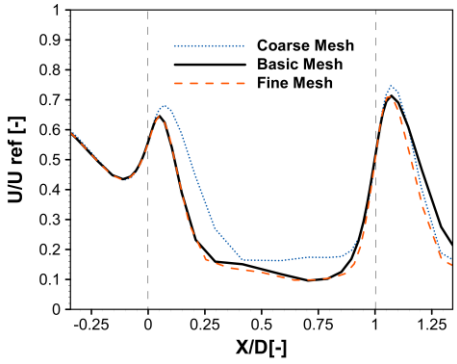

Figure5: Comparison between coarse mesh, basic mesh and fine mesh. Results show that basic mesh is sufficient.

Karava (2008) revealed the incident vertical profiles of mean wind speed and turbulent intensity based on wind tunnel measurements. The profile of mean velocity for inlet boundary condition simulation was based on obtained incident profiles. Blocken et al. (2007) found out Using incident profiles rather than approach profiles is important to have simulation accuracy. The inlet wind velocity profile was defined based on logarithmic law (Eq.1). U_{ABL} is a friction velocity equal to 0.35 m/s. k is a von_Karman constant equal to 0.42. The turbulence kinetic energy was calculated from (Eq.2) Where I_u is a turbulent strength or turbulent intensity which is calculated from one direction in wind tunnel experiment by Karava (2008). a is a parameter range from 0.5 to 1.5. Peren et al. (2015) found out a = 0.5 provided the best agreement with the experimental results in building with asymmetric positions.

Tominaga et al. (2008) proposed to use a = 1 and Ramponi and Blocken (2012) also found out a = 1 is the best value for buildings with symmetric opening positions. Therefore, in this study as the building has symmetric opening positions the value of parameter a in equ.2 is equal to 1. Turbulence dissipation rate (ε) and specific dissipation rate (ω) are defined by Eq.3 and Eq.4. where C is an empirical constant taken equal to 0.09. Figure 6.a shows the incident profiles of mean wind (U), turbulent kinetic energy (K) and turbulence dissipation rate (ω) at the inlet of the domain defined by Peren et al. (2015) while the parameter a is equal to 0.5. In this study Incident profiles of mean wind (U), turbulent kinetic energy (K) and turbulence dissipation rate (ω) at building position and in an empty domain are given in Figure 6.b. Sandgrain roughness is an important factor for wind profile accuracy. Blocken et al. (2007) derived Sandgarin roughness height based on aerodynamic roughness length Z_0 and roughness constant of 0.874 and based on Eq.5. Therefore, in this study Sandgrain roughness was taken equal to 0.28 mm.

$$U(z) = \frac{u_{ABL}}{\kappa} \ln\left(\frac{z+z_0}{z_0}\right) \quad (1)$$

Where:

U(z) = A speed in [m/s]; UABL = friction velocity in m/s; k = von-Karman constant equal to 0.42

$$K(z) = a\,(I_u(z)\,U(z))^2 \quad (2)$$

Where:

K(z) = turbulence kinetic energy in [m^2/s^2]; $I_u(z)$ = turbulent intensity in percent; U(z) = velocity at z height in m/s.

$$\varepsilon = u^{*3}_{ABL} / \kappa(z+z_0) \quad (3)$$

Where:

ε = turbulence dissipation rate in [m^2/s^3]; U_{ABL} = friction velocity in[m/s]; K(z) = turbulence kinetic energy.

$$\omega(z) = \varepsilon(z)/C_\mu\, K(Z) \quad (4)$$

Where:

ω = specific dissipation rate[m^2/s^3]; ε(z)= turbulence dissipation rate; C_μ = constant equal to 0.09. K(z) = turbulence kinetic energy in [m^2/s^2]

$$K_S = 9.793\, Z_0 / C_S \quad (5)$$

Where:

KS = Sand grain roughness; C_S = roughness constant; z_0 = height in meter [m].

a

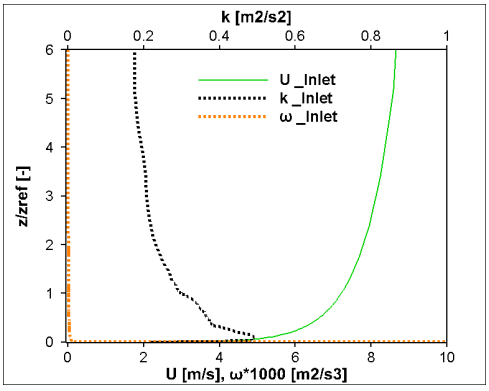

b

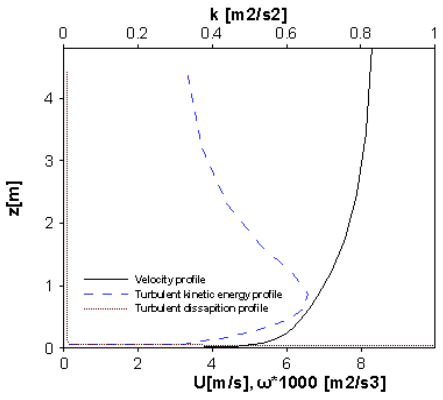

Figure 6: a.Inlet Velocity, turbulence kinetic energy and turbulence dissipation rate at the inlet of the domain defined by Peren et al. (2015) while a parameter is equal to 0.5. b.measured Velocity, turbulence kinetic energy and turbulence dissipation rate at building position in an empty domain while a parameter is equal to 1 and turbulence model is k-ω.

3.2.2. General CFD set up

All simulations were performed using ANSYS FLUENT 14. General simulation settings such as k-ω sst as a turbulence model was used. k-ω sst has the best agreement result for indoor natural ventilation. The commercially ANSYS FLUENT 14 software was used for the CFD simulation. The simulation governed by 3D dimensional Reynolds Averaged Navier_Stokes equations (RANS) in order to solve the steady-state governing equations in combination with turbulence model. The k- ω SST (shear-stress transport) was used as a turbulence model with standard wall function. The second-order upwind scheme was used for other governing equations and the "SIMPLE" (semi-implicit method for pressure-limited Equations) algorithm for the pressure_ velocity coupling was performed. The Simulations were run in steady-state mode with the convergence criteria of 10^{-6} for x and y momentum, 10^{-5} for z momentum, and 10^{-4} for k, ε and continuity. The results observed over 9800 iterations. The oscillator convergence was observed. Ramponi and Blocken (2012)also found an oscillator convergence simulation of cross-ventilation flow for different isolated building configurations. In order to evaluate a constant value in oscillatory variations, the average of 800 iterations (between 9000 and 9800 iterations) for pressure and velocity were calculated.

3.3. Compare to experimental data

The results show that the CFD setup simulation has good agreement with experimental wind tunnel data by Karava (Figure7.a).

a **b**

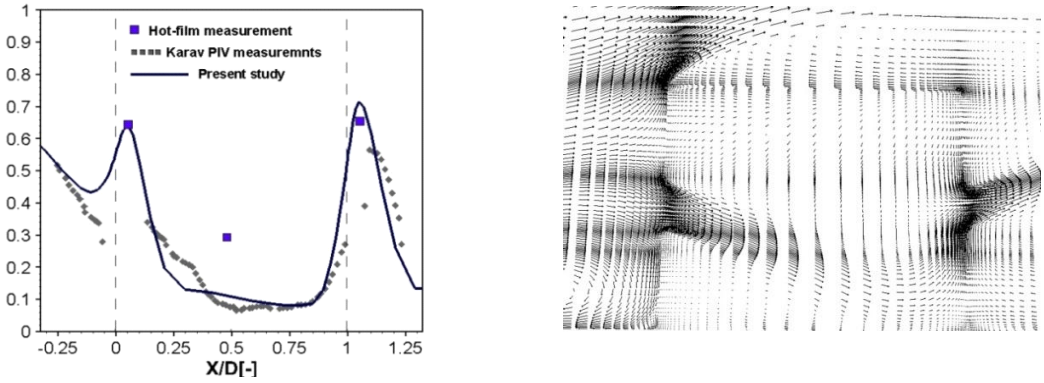

Figure 7: a. Comparison of the mean wind velocity from the wind tunnel experiment and CFD simulation at defined AB line. the result shows a good agreement with experimental data. b.the velocity vectors in CFD simulation.

3.4. Domain dimensions Independent test

The scale experimental model does not replicate other geometries considered in this study. Adding a breezeway at the back of the model change the aspect ratio of the validated model, this aspect ratio minimizes the distance for the air to flow. To not affect the results, a sensitivity analysis on the boundary condition has been conducted. The cube model was tested in new computational domain size with 0.9m × 0.48 m× 1.58 m in 1:200 reduced scale. The domain was expanded at the downstream of 15H to indicate that the results are independent from the downstream domain size. Figure 8 shows the comparison between indoor mean velocity at the defined AB line of the base model in domain size of 0.9 m × 0.48 m × 1.54 m and domain size of 0.9m × 0.48 m × 1.58 m. The

results indicate that the domain size becomes independent. Therefore, the new domain was simulated for all the models with breezeway.

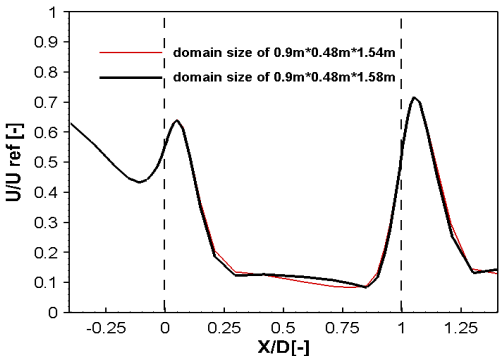

Figure 8: Analysis of domain size independence for two different boundary sizes.

4. The effect of breezeway width on indoor natural ventilation

Simulations were conducted to model the effect of breezeway shaft depth on indoor airflow. Four different geometries with a fixed stilt height and different breezeway depth were analyzed. Geometry “a” is a cubic model based on the experimental model with an elevated floor of the ground. Other three geometries “b”, “c” and “d” are the same model with an elevated floor connected to a 0.049 meter height breezeway without any obstructions. Simulation “a” served as a baseline case to compare against other simulations. The volume of all these models kept constant and equal to 0.7cm^3 in reduced scale. The cubic model has a 0.1m depth, 0.1 m width, and 0.07 m height. In case b, c and d the breezeway shaft is modeled with cross sectional area of 0.000392m^2, 0.00098 m^2 and 0.00196 m^2, respectively. All four cases have an equal elevated floor height of 0.01m in reduce scale corresponds to 2m in full scale (Figure9).

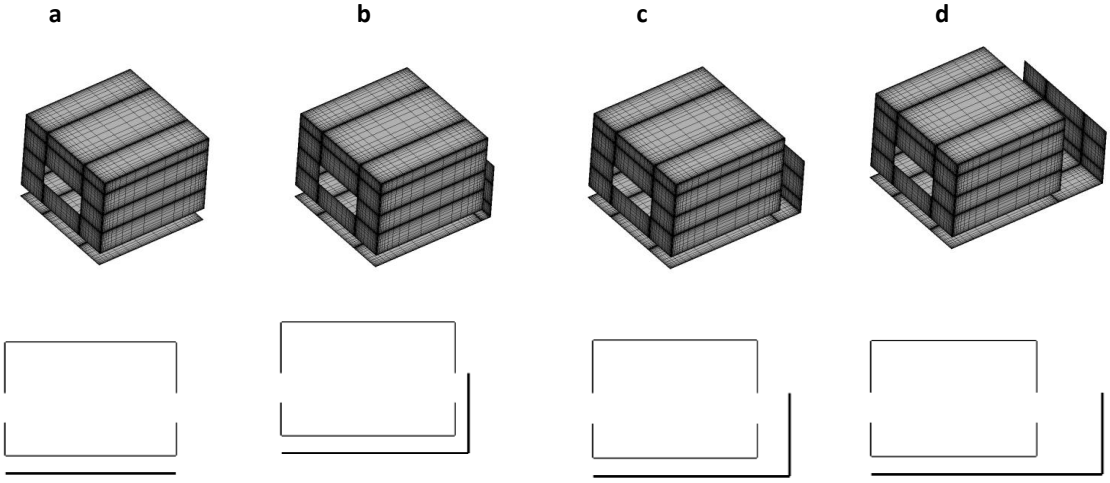

Figure 9: Four different geometries were simulated

Four models were analyzed and compared with each other at the defined line in the middle of the windward and leeward opening. Experimental set up is mentioned in chapter 3, and is used for conducting simulations. The goal of this section is to understand the effect of breezeway shaft depth in indoor airflow. Velocity and pressure

contours are shown in Figure.5. As it is shown Results from small scale simulation suggest that the breezeway shaft at the backward of the building impact the airflow inside the building.

The air pathway bends toward the breezeway shaft opening. As it is shown, as the breezeway shaft expands (model d), more airflow into the breezeway shaft. This corresponds with a pressure loss at the leeward façade. Pressure loss in breezeway shaft leads to a larger pressure difference between windward and leeward opening and increase indoor flow rate. In model b and c due to a lower breezeway width, the airflow couldn't pass easily in the breezeway shaft. The air turned into small wakes which cause lower air velocity in the shaft and increase pressure at the back of the model. The measured pressure coefficient for all the models is presented in table1.

Table 1: Pressure differences between windward and leeward facades of building models

Model	P coefficient windward opening	P coefficient leeward opening	ΔP
a	0.87	0.07	0.8
b	0.9842	0.033	0.6542
c	0.9	0.16	0.74
d	0.86	0.03	0.83

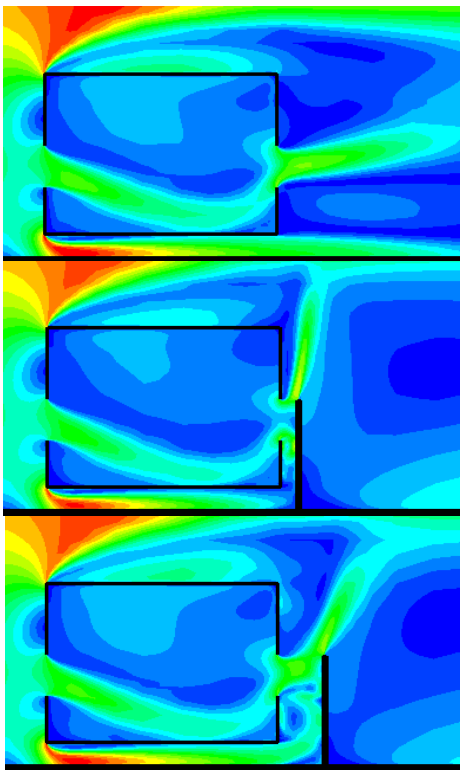

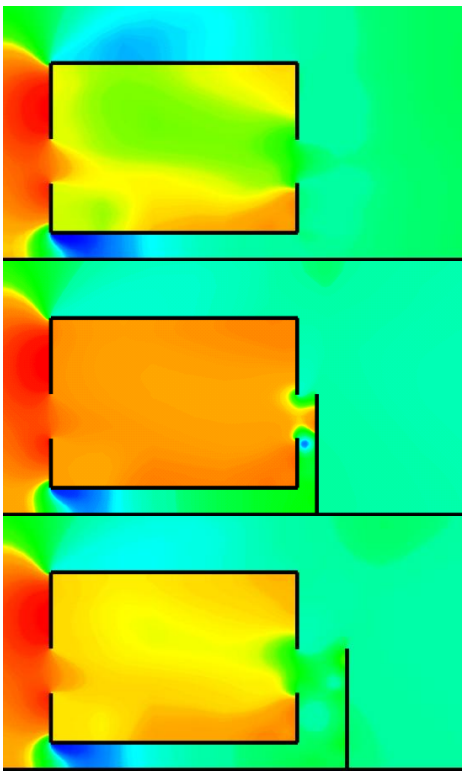

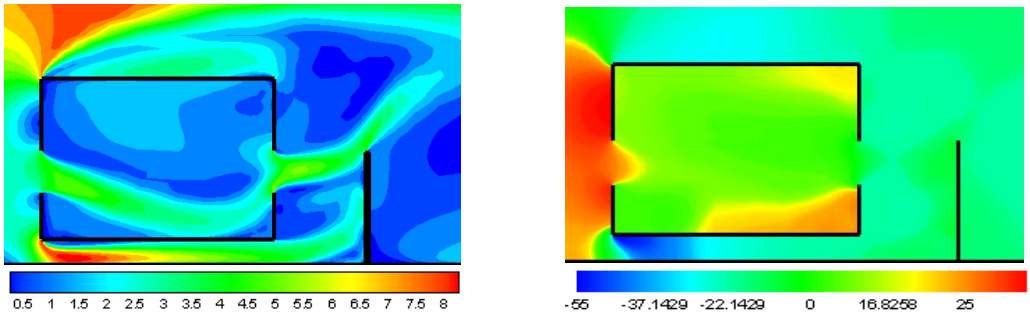

Figure10. Velocity contours and pressure contours along the middle plane for geometry a,b,c and d. contours indicate the air entering the building through the crawl space under the building and first floor and exit from the breezeway shaft.

5. Conclusion

Results from small scale simulation suggest that the breezeway shaft at the backward of the building impact the airflow inside the building. Figure 11.a indicates comparison between indoor mean wind velocity along the defined horizontal line (AB) at the middle of the windward and leeward opening in all four models. As it is shown compare to the base model (a model without breezeway shaft), the mean wind velocity along the horizontal line is 30% and 10% lower in model “b” and “c”, respectively. In model “d” mean wind velocity along the horizontal line increases 3% compare to the base model. As the breezeway width increases, the indoor air velocity increases. Figure11.b shows the differences in indoor airflow rates between all four models. pressures were measured at the windward and leeward openings. As it is shown model “d”, has the highest indoor airflow rate compare to other models. Model “d “compare to models “b “and “c “increases indoor airflow rate 12% and 8% respectively. Model “b “has the lowest airflow rate, compare to all the other models. Compare to the model without the breezeway (model a), models “b“and “c“ decreases indoor airflow rate 10% and 4% respectively. This study suggests that the aspect ratio of 1-meter breezeways used in low rise traditional buildings in the north of Iran had a negative effect on indoor airflow.

a **b**

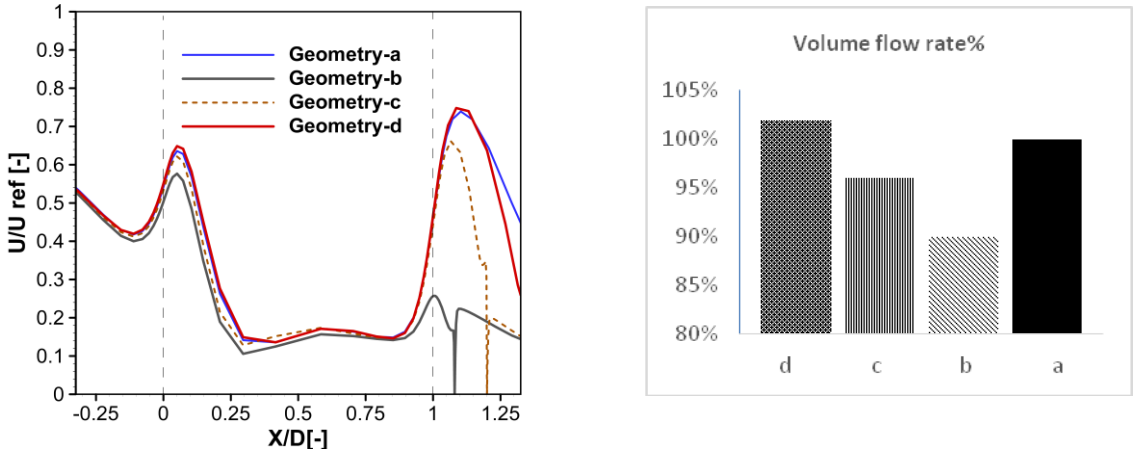

Figure 11- Comparison of mean wind velocity and indoor volume flow rate between four different models

This study investigated the effect of breezeway width on indoor natural ventilation in an elevated building with symmetric opening positions. However, there are a number of limitations that can be studied in future researches. First of all, the effect of the side yard wasn't taken into account in this research, even though it is an important factor and has an effect on indoor natural ventilation. Secondly, the model was adiabatic and the effect of temperature on this system wasn't analyzed. There is also a need for analysis on further building aspect ratios in order to understand the effect of elevated floor height on indoor natural ventilation. Overall, the backyard breezeway width is an important factor in design for an appropriate indoor natural ventilation. The backyard breezeway wall should be placed at the correct distance from the building wall in order to increase indoor airflows.

References

Blocken, B., Stathopoulos, T., & Carmeliet, J. (2007). CFD simulation of the atmospheric boundary layer: wall function problems. *Atmospheric Environment, 41*(2), 238-252. doi:https://doi.org/10.1016/j.atmosenv.2006.08.019

Chu, C.-R., & Chiang, B.-F. (2014). Wind-driven cross ventilation in long buildings. *Building and Environment, 80*, 150-158. doi:https://doi.org/10.1016/j.buildenv.2014.05.017

Franke, J., Hellsten, A., Schlünzen, H., & Carissimo, B. (2007). *BEST PRACTICE GUIDELINE FOR THE CFD SIMULATION OF FLOWS IN THE URBAN ENVIRONMENT*. Retrieved from Brussels:

Holmes, J. D. (1994). Wind pressures on tropical housing. *Journal of Wind Engineering and Industrial Aerodynamics, 53*(1-2), 105-123. doi:https://doi.org/10.1016/0167-6105(94)90021-3

Karava, P. (2008). *Airflow prediction in buildings for natural ventilation design: wind tunnel measurements and simulation* (Ph.D.). Concordia University,

Kosutova, K., Hooff, T. v., Vanderwel, C., & Blocken, B. (2019). Cross-ventilation in a generic isolated building equipped with louvers: Wind-tunnel experiments and CFD simulations. *Building and Environment, 154*, 263-280. doi:https://doi.org/10.1016/j.buildenv.2019.03.019

Montazeri, H., & Blocken, B. (2013). CFD simulation of wind-induced pressure coefficients on buildings with and without balconies: Validation and sensitivity analysis. *Building and Environment, 60*, 137-149. doi:https://doi.org/10.1016/j.buildenv.2012.11.012

Perén, J. I., Hooff, T. v., Leite, B., & Blocken, B. (2015). Impact of eaves on cross-ventilation of a generic isolated leeward sawtooth roof building: Windward eaves, leeward eaves and eaves inclination. *Building and Environment, 92*, 578-590. doi:10.1016/j.buildenv.2015.05.011

Ramponi, R., & Blocken, B. (2012). CFD simulation of cross-ventilation flow for different isolated building configurations: Validation with wind tunnel measurements and analysis of physical and numerical diffusion effects. *Journal of Wind Engineering and Industrial Aerodynamics, 104-106*, 408-418. doi:https://doi.org/10.1016/j.jweia.2012.02.005

Tantasavasdi, C., Srebric, J., & Chen, Q. (2001). Natural ventilation design for houses in Thailand. *Energy and Buildings, 33*(8), 815-824. doi:https://doi.org/10.1016/S0378-7788(01)00073-1

Tominaga, Y., Akabayashi, S.-i., Kitahara, T., & Arinami, Y. (2015). Airflow around isolated gable-roof buildings with different roof pitches: Wind tunnel experiments and CFD simulations. *Building and Environment, 84*, 204-213. doi:https://doi.org/10.1016/j.buildenv.2014.11.012

Tominaga, Y., Mochida, A., Yoshie, R., Kataoka, H., Nozu, T., Yoshikawa, M., & Shirasawa, T. (2008). AIJ guidelines for practical applications of CFD to pedestrian wind environment around buildings. *Journal of Wind Engineering and Industrial Aerodynamics, 96*(10-11), 1749-1761. doi:https://doi.org/10.1016/j.jweia.2008.02.058

Perén, J. I., Hooff, T. v., Leite, B., & Blocken, B. (2015). CFD analysis of cross-ventilation of a generic isolated building with asymmetric opening positions: Impact of roof angle and opening location. Building and Environment, 85, 263-276. doi.org/10.1016/j.buildenv.2014.12.007

Tominaga, Y. Blocken, B. (2015). Wind tunnel experiments on cross-ventilation flow of a generic building with contaminant dispersion in unsheltered and sheltered conditions. Building and Environment, 92, 452-461. doi.org/10.1016/j.buildenv.2015.05.026